Comparison of LS-DYNA and NISA in Solving Dynamic Pulse Buckling Problems in Laminated Composite Beams

Haipeng Han and Farid Taheri
Department of Civil Engineering, Dalhousie University
Halifax, NS Canada B3J 1Z1

Abstract

In this paper the dynamic pulse buckling of laminated composite beams was analyzed using LS-DYNA and another widely used commercial FE code, namely NISA (Ver.12), developed by EMRC (Engineering Mechanics Research Corp). Two types of impact loadings that could induce dynamic pulse buckling of composite beams were analyzed. The first one was a force applied to the structure in a very short duration (i.e., an impulse load). The other one was the impact of a moving mass having a certain initial velocity.

This problem brings considerable challenges if one is to simulate the phenomenon accurately. The main objective of this technical exercise was to investigate the influence of certain numerical parameters on the integrity of the out coming results. The objective was also to assess the performance of a "conventional, general purpose" type FEM program versus LS-DYNA, which is considered as a leading FEM code for the analysis of highly nonlinear phenomena. This was an interesting exercise in demonstrating why one should use codes like LS-DYNA, as oppose the general purpose FEA codes when considering such highly non-linear phenomena.

Both abovementioned loading types were considered in this study. In the analysis using LS-DYNA, the force function was introduced by applying an impulse force at one end of the FRP beam. The moving object was also modeled in LS-DYNA by means of a rigid wall having a mass and an initial velocity. The impact by moving object could not be accommodated by NISA, so only the pseudo-impulse type loading could be considered in NISA. Parametric studies were also conducted to investigate the effect of the slenderness ratio, the curvature and the stacking sequences of the FRP beams, as well as the examination of the influence of the initial imperfection used to promote structural instability.

Keyword: Composites, beams, axial impact, pulse buckling, finite element, sensitivity analysis.

1. Introduction

Dynamic pulse buckling is a dynamic instability phenomenon, in which the excessive growth of the lateral or out of plane displacement results from a transient loading function in the form of a single pulse with a magnitude greater than that of the static Euler buckling load [1]. Most researchers have investigated the dynamic buckling and postbuckling of structures subject to in-plane or transverse periodic load. Only a few works have considered the dynamic pulse buckling of structures subject to axial impulse loading [2, 3].

Zukas et al [4] proposed the three major steps in studying the response of structural impact, including determination of: (1) the impact-induced surface pressure and its distribution, (2) the internal stresses in the structures caused by the surface pressure, and (3) determination of failure modes in the structures caused by the internal stresses. In the pulse buckling analysis of FRP beam subject to axial impact, the analysis steps are as follows: (i) evaluation of the internal force induced by the impact at the impacted end of beam, (ii) analysis of the dynamic response of beam subjected to the induced internal force, and (iii) analysis of the dynamic buckling behaviour. Numerical integration is used to solve the dynamic response in the second step. There are two categories for direct integration methods, namely explicit and implicit, which are commonly used in most commercial finite element codes. For example, an explicit method is used in the explicit analysis of LS-DYNA and the Newmark method is used in NISA for dynamic analysis. As discussed in [2], in the event of short duration impact, the damping does

not play a significant role as the maximum response is reached before much energy is dissipated through damping. Therefore damping effect is neglected in this type of analysis.

Using the Timoshenko beam assumption and considering the axial, flexural, and rotation inertias and through thickness shear deformation of laminated composite beam, Zhang [3] used the following equilibrium governing equations for the analysis of the dynamic pulse buckling of a FRP beam and solved them using finite difference method (FDM).

$$\frac{\partial N_x}{\partial x} - I_1 \frac{\partial^2 u}{\partial t^2} = 0 \tag{1}$$

$$\frac{\partial (N_x (\theta - \frac{\partial w_0}{\partial x}))}{\partial x} - \frac{\partial V}{\partial x} + I_1 \frac{\partial^2 w}{\partial t^2} = 0 \tag{2}$$

$$-\frac{\partial M_x}{\partial x} + V + I_2 \frac{\partial^2 \theta}{\partial t^2} = 0 \tag{3}$$

where $w_0(x) = W_0 \sin(\pi x / l)$ is the initial geometric imperfection. The unknowns $u(x,t)$, $w(x,t)$ and $\theta(x,t)$ are the axial and the lateral deflection and rotation of cross section of the beam, respectively. Equations (1-3) apply to the fixed-end or pinned-end supported FRP beam subject to (i) an impulse force function ($F(t)$) or (ii) a pulse generated by a moving mass (M) with an initial velocity of (V_0).

The following sections present the case studies corresponding to these two types of impact loadings, which will demonstrate the capabilities of the two codes.

2. Case study #I

Problem Description

An 8-layer glass/epoxy laminated composite beam with a fixed boundary condition is subject to an impact by a moving mass, as shown in Figure 1.
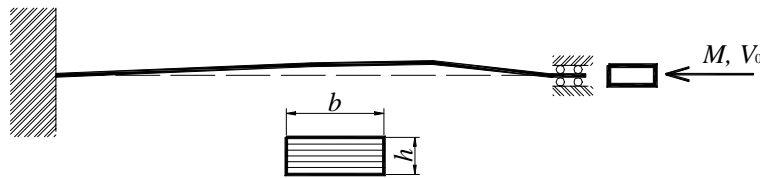
Figure 1: Slender fixed -fixed beam impacted by a moving mass

The initial geometric imperfection is assumed to be of a half-sine wave nature. Several types of geometric imperfections were introduced by selecting different factors in the equation $W_0 = factor \times h$. The geometrical and material properties are listed in below:

$$b \times h \times L = 20mm \times 1.6mm \times 300mm, \ E_{11} = 39 \times 10^3 MPa, \ E_{22} = 8.9 \times 10^3 MPa, \ G_{12} = 3.8 \times 10^3 MPa, \ \gamma_{12} = 0.28 \text{ and}$$
$$\rho = 2100 Kg / m^3.$$

2.1 Summary of modeling in LS-DYNA

Both 3-D and 2-D models were constructed for these problems. The fully integrated quadratic 8-node solid element with nodal rotation and the Belytschko-Tsay shell element were employed in the 3-D and 2-D models, respectively, to simulate the response of the FRP beam.

Several material models were also investigated for modeling the laminated composite material, and the MAT_COMPOSITE_DAMAGE (No.22 in the library) was found to be the most suitable one.

Having gone through this exercise, it was discovered that the use of the solid elements for modelling the laminated composite beam was not a straightforward task, because one must use at least one layer of elements for each layer (lamina). This would result in a formidably huge and uneconomical model. However, since the micro failure of the materials is not of primary interest in this study, therefore the shell elements could be used to analyze the FRP. In this case, for verification, only a ($[0^0]_8$) FRP beam was modeled using the 3-D elements.

The impacting moving mass was modeled as a rigid wall defined by keyword *RIGIDWALL_PLANAR_MOVING_FORCES. Moreover, the keyword *CONTACT_ AUTOMATIC_SINGLE_SURFACE was used to prevent the self penetration during the impact, in which the static and dynamic coefficient of friction were chosen as fs=fd=0.01. The rigid wall was used as a master surface and the beam end was used as a slave surface. A FORTRAN code was developed to generate the nodal coordinates of the initial geometric imperfection with a half sine wave shape.

2.2 Summary of modeling in NISA

The pulse buckling analysis of FRP beam was also conducted with another commercial finite element code NISA (Ver.12), developed by EMRC. Only the FRP beam with $[0^0]_8$ stacking sequence and the initial geometric imperfection of $w_0 = 0.1h$ was considered in NISA. Three keywords *RCTABLE, *LAMANGLE and *LAMSEQ were used to model the laminated composite beam using NISA's shell element (NKTP=32).

As stated, the first step in analyzing the impact events would be to determine the contact force between the two bodies involving in the impact (a time dependent function). Such a force function is also dependent on the material property of the two contacting bodies and the contacting surfaces' conditions. The second step would be to find the dynamic response of the impacting bodies by conducting a dynamic analysis. As NISA does not have a robust and extensive contact algorithms, one would have to determine the force function before conducting the linear direct transient analysis. Two approaches were attempted in NISA to tackle this problem: in the first approach, the force function was extracted from the results of LS-DYNA's contact analysis, as will be discussed later in detail. In the second approach, the moving mass was modeled as a concentrated mass element with certain initial velocity attached to the impacted end of the FRP beam.

2.2.1 Approach I

The linear direct transient analysis was conducted using the Newmark method with the default values of β and γ. Firstly, the axial compressive stress's history, σ_{DYNA}, at the impact end was extracted from the results obtained in LS-DYNA. Figure 2 shows the history of the compressive axial stress. One can also approximate the stress wave as a half-period sine wave [5].

$$P(t) = \begin{cases} P_0 \sin\left(\dfrac{\pi t}{t_0}\right) & 0 \le t \le t_0 \\ 0 & t \ge t_0 \end{cases} \tag{4}$$

This stress is then converted to an axial force function by $F(t) = \sigma_{DYNA}bh$, where b and h are the width and thickness of the beam, respectively. Finally, this force function was applied consistently at the impacted end of beam in NISA model.
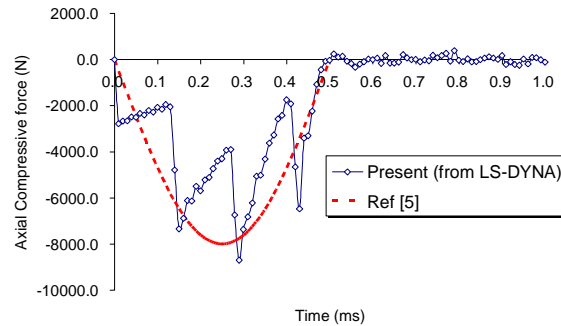
Figure 2: Time history of the compressive stress at the impacted end of beam

2.2.2 Approach II

The 3-D point mass element (NKTP=26) was used to simulate the moving mass with certain initial velocity. In this approach, the mass elements were superimposed on the nodes forming the impacted end boundary of the FRP beam, and an initial velocity was assigned to these nodes (or the masses). A linear direct transient analysis was conducted for this model. Different combinations of mass and velocity (creating the same momentum) were tried in the analyses to evaluate the influence of the mass and velocity.

2.3 Results and discussion

The results obtained from LS-DYNA and NISA are compared in this section. Figures 3 shows the response history of axial displacement at the impact end, the mid-span deflection and compressive microstrain at the mid-span of beam obtained from LS-DYNA and approach I in NISA.

(a)   (b)   (c)
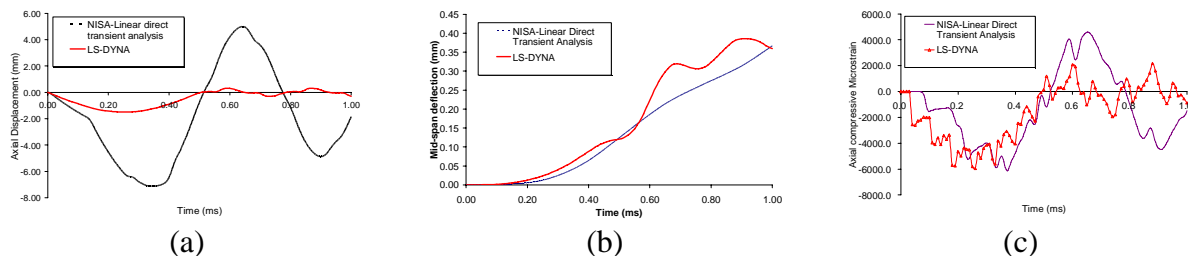
Figure 3: Response history of the axial displacement, mid-span deflection and compressive strain at beam's mid span obtained from LS-DYNA and NISA-Approach I

It is obvious that the difference in the magnitudes of the displacement is significant, despite the fact that both codes produce approximately similar lowest wave frequencies and some higher wave frequencies. The results indicate that NISA could only produce reliable results if the force function is known. As for the mid-span deflection, similar magnitudes were obtained from NISA and LS-DYNA. However, NISA could not reflect the lateral wave propagation; therefore, it would not be suitable for tackling dynamic pulse buckling problem, in which an

axial impact would induce a lateral wave propagation, which in turn would increase the lateral deflection, hence reducing the compressive strain. In a dynamic pulse buckling analysis, the lateral deflection is one of the most important indicators of the structure's response; NISA cannot accurately capture the variation of this indicator. Furthermore, although similar profile and low-mode response are observed from these two FE codes, but significantly large difference of compressive strain and high-mode response was observed. It is therefore concluded that NISA would not be a suitable code for dynamic pulse buckling analysis.

In the second analysis approach in NISA, the moving mass was modeled using the concentrated mass element (3-D point mass, NKTP=26) with an initial velocity. This approach was found to be unsuccessful. The major problem was observed to be that the addition of mass to the beam's end significantly influenced the intrinsic property of the structure system (i.e., its natural frequency). In an attempt to resolve this deficiency, several combinations of mass and initial velocity were considered while maintaining the same momentum (e.g. 0.1 Kg x 10 m/s, 0.01 Kg x 100 m/s, etc). Figure 4 shows the results of some of the cases analyzed. As seen, the desired consistency could not be achieved. It is therefore concluded that this approach is not a suitable one for conducting pulse buckling analysis.
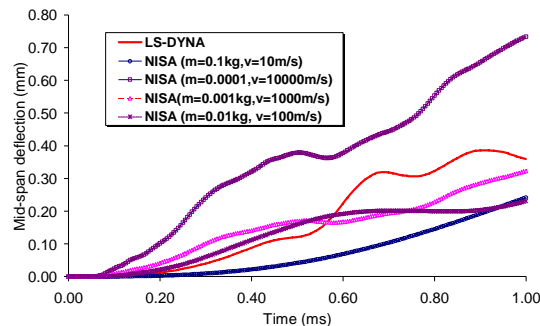
Figure 4 Comparison of the mid span deflection obtained from LS-DYNA and NISA (using the second Approach)

As discussed above, although the output of the contact analysis conducted in LS-DYNA was imported into the NISA model, NISA still was not able to produce satisfactory results. Therefore the additional parametric studies were all carried out by LS-DYNA. It should be noted that the above analysis approach and results were only for the dynamic case in which the FRP beam was subjected to a certain impact energy (i.e., $m=0.1Kg, v_0=10m/s$). To better understand the pulse buckling response, the FRP beam was subjected to various impact energies. Figure 5a shows the mid-span deflection history of the unidirectional FRP beam at various impact velocities. The results indicate that when the impact velocity exceeds some 'critical' value (in this case 14m/s), the mid span deflection would significantly increase, while the axial displacement and compressive strain of the beam remain relatively constant. Therefore, an impulse at such critical velocity would cause pulse buckling of such beams. For the case of the constant moving mass, when the impact momentum (product of mass and velocity) increased from zero to some critical value, the maximum lateral deflection was significantly increased, as illustrated in figure 5b.
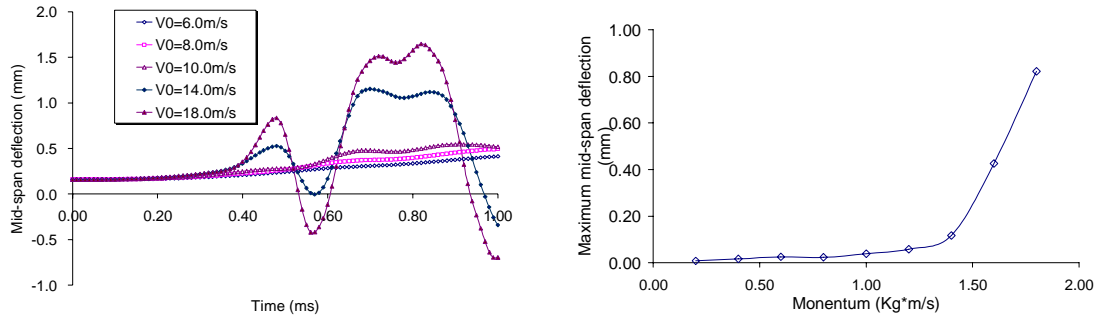
(a) Comparison of the mid-span deflection at different impact velocities

(b) Maximum Mid-span deflection versus impact momentum

Figure 5: Pulse buckling of unidirectional epoxy/glass beam with an initial geometric imperfection of $W_0 = 0.01h$

2.4 Parametric studies

Parametric studies using LS-DYNA were carried out to investigate the effect of the initial imperfection, slenderness ratio, and various stacking sequences on the pulse buckling response of FRP beams.

2.4.1 Initial imperfection

Figure 6 shows the variation of maximum mid-span deflection with respect to increasing momentum for beams with different initial imperfection amplitude. It shows that the larger imperfection amplitude results in a small critical momentum of impact. As seen, the beam with the 0.001h imperfection exhibited a much higher critical momentum (about 1.6 Kg*m/s) than the one with 0.1h imperfection (1.0 Kg*m/s).
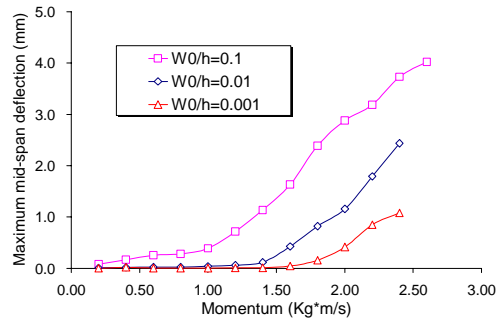
Figure 6: Maximum mid-span deflection vs. momentum for FRP beam with different initial imperfection amplitudes

2.4.2 Slenderness ratio influence

Three different lengths (450mm, 300mm and 150 mm) FRP beams with the same thickness and width were analyzed to study the influence of slenderness ratio on the pulse buckling response of the FRP beams. The beams also had three different magnitudes of imperfection (i.e., 0.1h, 0.01h and 0.001h). Figure 7 shows the plot of the slenderness ratio versus critical momentum for the beams. It is observed that the more slender the beam is, the more momentum the FRP beam can endure. This phenomenon is contradicts the common sense as far as the static buckling of a beam is concerned, in that, the smaller the slenderness ratio, the more the buckling capacity. The reason is postulated to be due to the fact that for each group of beams having the same imperfection amplitude, the shorter the beam the more its curvature.

When such a beam is subjected to an impulse, the less slender beam becomes subjected to a larger bending moment than the more slender ones, thus causing a larger deflection in the shorter beams.
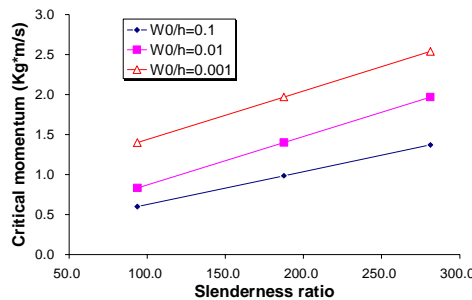
Figure 7: Critical buckling momentum as a function of slenderness ratio for beams with different type of imperfections

2.4.3 Influence of laminate's stacking sequence

FRP beams of the same thickness but with various stacking sequences, including $[0^0]_8$, $[0^0/90^0]_{2s}$, $[\pm45^0]_{2s}$ and $[\pm22.5^0]_{2s}$ were analyzed. Figure 8a shows the normalized axial displacement response at the impacted end of the FRP beams. Figure 8b shows the normalized maximum mid-span deflection response versus impact momentum for the FRP beams. It is observed that the $[0^0]_8$ beam has the highest capacity of impact momentum, while the $[\pm45^0]_{2s}$ beam has the lowest. The values of the flexural stiffness of the beams, as well as the onset of pulse buckling have also been tabulated in Table 1. The common sense dictates that the stiffer the beam, the lower its axial and mid-span deflections; nonetheless, the variations in the displacements are not in proportion to the variation in the beams' stiffness. Moreover, as the values in Table 1 indicate, although the onset of pulse buckling is a function of the beams' stiffness, but it is not a linear function. Note that this principle may only apply to the symmetrically stacked laminated FRP beams.

(a) Normalized axial displacement history at impact end

(b) Normalized maximum mid-span deflections vs. momentum
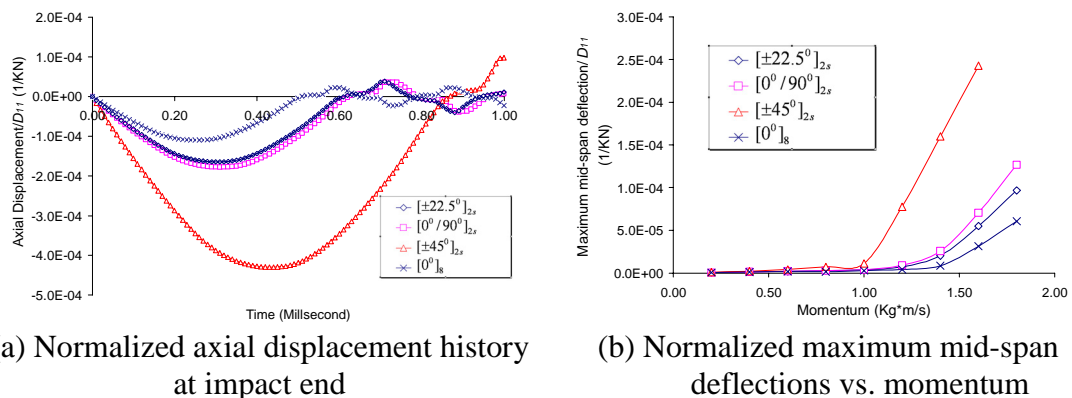
Figure 8: Pulse buckling response of FRP beams with various stacking sequences

Table 1 Flexural stiffness and onset of pulse buckling momentum for FRP beams with various stacking sequences

Laminates	$[0^0]_8$	$[0^0/90^0]_{2s}$	$[\pm45^0]_{2s}$	$[\pm22.5^0]_{2s}$
D_{11} (KN.mm)	1.355×10^4	1.029×10^4	0.589×10^4	1.081×10^4
Momentum (Kg*m/s)	1.35	1.16	1.00	1.19

3. Case Study #2

Problem description

A simply supported 8-layer unidirectional, $[0^0]_8$, Kevlar/epoxy laminated beam is impacted by a rectangular impact force as shown in Figure 9.
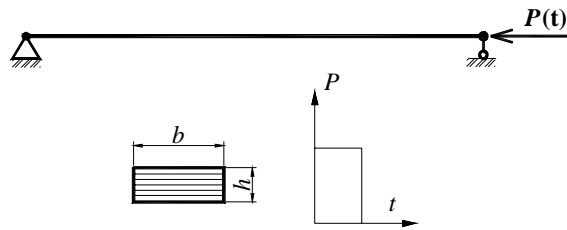
Figure 9: Slender beam is impacted by an impulse

The initial geometric imperfection is assumed to have a half-sine wave $W_0 = 0.1h\sin(\pi x/l)$. The geometrical and material properties are listed as below:

$$b\times h\times L = 12.7mm\times0.3725mm\times762mm, \ E_{11}=87\times10^3 MPa, \ E_{22}=5.5\times10^3 MPa, \ G_{12}=2.2\times10^3 MPa, \ \gamma_{12}=0.34 \text{ and}$$

$$\rho=1380 Kg/m^3.$$

3.1 Summary of modeling

A 2-D model was also constructed for this problem in LS-DYNA. The analysis detail is similar to the previous case study; the only difference was the type of impulse used in modelling the load condition. In this case a rectangular pulse applied to the impacted end of the FRP beam. Explicit analysis was conducted to get the dynamic response of the FRP beam.

In NISA, the same type of analysis was conducted as in the first approach described in the previous section. The only difference was that the force function was a known impulse force function. Again, a FORTRAN program was written to generate the geometrical imperfection of the FRP beam for promotion of instability.

In this study, it was found it is very important to set appropriate time duration for the impact event in the analysis. Usually the time interval is dependant on the natural period of the structure. In this analysis, the total duration of the event for the compressive wave to propagate from the impacted end of the beam to the other end was set at 10 times of the natural period of the beam. This would ensure that the pulse buckling response of the beam would be accurately captured without excessive computation effort. The propagation speed for the compressive wave in the FRP beam was calculated by [3]:

$$c = \sqrt{\frac{A}{I_1}}$$

(5)

where

$$A = \int_{-h/2}^{h/2} Q_{11} dz = \sum_{k=1}^{n} Q_{11}^k (h_k - h_{k-1}) \tag{6}$$

$$I_1 = \int_{-h/2}^{h/2} \rho dz = \sum_{k=1}^{n} \rho (h_k - h_{k-1}) \tag{7}$$

Therefore, the propagation speed was estimated at c=7625 m/s, giving $t_1 = l/c$ $= 0.762/7625 \approx 1.0 \times 10^{-4} s$ for the wave to propagate through the beam. Thus an event duration of $t = 10 t_1 \approx 1 \times 10^{-3} s$ was selected. To ensure accurate dynamic computation, the time step was set as 10^{-6} s, which is one thousandth of the total duration of the event.

3.2 Results and discussion

  Figure 10 shows the response history of the axial displacement at the impacted end of the FRP beam obtained from both NISA and LS-DYNA. The results from LS-DYNA were proven to be reasonably accurate in comparison to the results obtained from the 3D analysis. As shown in the figure, the response histories obtained from the two FE codes are reasonably comparable in magnitude, and the two codes produce almost the same dominant period. The differences in the magnitude and the visible high vibration mode are attributed to the nature of the elements used in the two codes. The Belytschko-Tsay shell element of LS-DYNA adopts an hourglass algorithm to accommodate the appropriate bending effect, whereas this algorithm is not available in NISA. Figure 11 shows the stress wave propagation at different stations along the beam obtained by NISA and LS-DYNA. As stated previously, the time for the stress travel through the beam was estimated to be approximately $1.0 \times 10^{-4} s$ (as also seen in Figure 11). These two figures demonstrate that NISA performs reasonably well on the pulse buckling analysis in which the impact is induced by a pulse force.

  As mentioned before, the dynamic pulse buckling occurs when the magnitude of impact pulse exceed some critical value. In this problem, for a constant force, when the time duration of the force approaches to a critical value, after which a small increase in the duration would induce a significant increase in the transverse deflection of the beam, while the axial load capacity would not increase significantly, as shown in Figure 12.
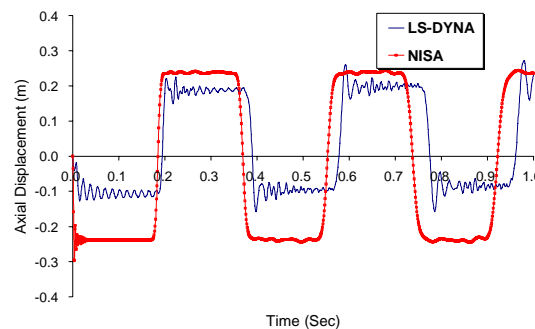
Figure 10: Axial displacement at the impacted end of the simply supported FRP beam obtained from NISA and LS-DYNA
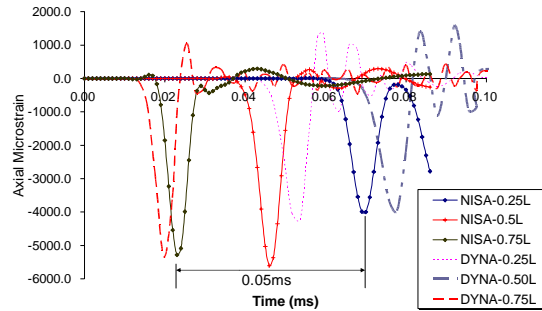
Figure 11: Compressive strain wave propagation of the simply supported beam obtained from NISA and LS-DYNA
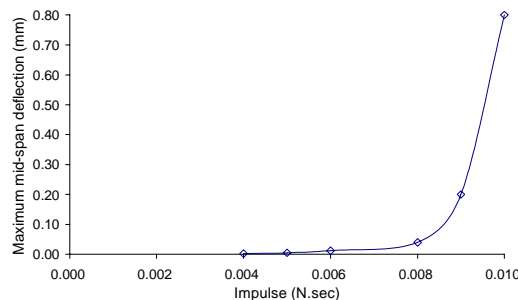
Figure 12: Plot of the Maximum Mid-span deflection versus impulse response of the Kevlar/epoxy beam with initial imperfection

4. Concluding remarks

In this paper the dynamic pulse buckling of laminated composite beams was analyzed using LS-DYNA and another widely used commercial FE code, namely the NISA (Ver.12), developed by Engineering Mechanics Research Corp. The main objective of this computational exercise was to investigate the influence of certain parameters on the integrity of the out coming results. The objective was also to measure the performance of a "conventional, general purpose" type FEM program, and LS-DYNA, which is considered as a leading FEM code for the analysis of highly nonlinear phenomena. This was an interesting exercise in demonstrating why one should use codes like LS-DYNA, as oppose the general purpose FEA codes when considering the dynamic pulse buckling analysis of FRP beam.

Two types of impact loadings were investigated in this study. In the analysis using LS-DYNA, the force function was introduced by applying an impulse force at one end of the FRP beams. The impact by a moving object was also modeled in LS-DYNA by means of modelling a rigid wall having a mass and an initial velocity. The above loadings type could not be accommodated by NISA, so only the pseudo-impulse type loading could be considered in NISA. The comparison of results obtained from NISA and LS-DYNA showed that NISA could be successfully used in analyzing a class of pulse buckling problems in which impact could be modelled as an impulse. However, as NISA does not offer a suitable contact algorithm, the code is not suitable for the class of pulse buckling problems, in which the impact is induced by a moving mass.

A dynamic buckling criterion was also established for both types of impact loadings. It was postulated that when the momentum or the impulse reaches a certain critical value, a small increase in impact velocity or the duration of the pulse force would induce a significant increase in the lateral deflection of the beams. A detailed parametric study was also carried out by LS-DYNA in consideration of the influence of slenderness ratio, the initial geometric imperfection and the stack sequence on the dynamic pulse buckling response of the FRP beam.

Acknowledgement

References

[1] Ari-Gur J., Weller T. and Singer J., Experimental and theoretical studies of columns under axial impact, *International Journal of Solids Structures*, Vol 18 619-641, 1982

[2] Kenny S., Dynamic pulse buckling of slender beams with geometric imperfection subjected to an axial impact, *PhD thesis*, Dalhousie University, 2001

[3] Zhang Z., Investigation on dynamic pulse buckling and damage behaviour of composite laminated beam subjected to axial impulse, *PhD thesis*, Dalhousie University, 2004

[4] Zukas J.A., Nicholas T. Swift, H.F., Greszczuk, L.B. and Curran D.R., Impact dynamics, Krieger Publishing Company, Malabar, Florida, 1992

[5] Hao H., Cheong H.K. and Cui S., Analysis of imperfect column buckling under intermediate velocity impact. *International Journal of Solids and Structures*, 37: 5297-5313, 2000